RhoA/Rho Kinase Signaling in the Cumulus Mediates Extracellular Matrix Assembly

Rieko Yodoi,* Shigero Tamba,* Kazushi Morimoto,* Eri Segi-Nishida, Mika Nishihara, Atsushi Ichikawa, Shuh Narumiya, and Yukihiko Sugimoto

Department of Physiological Chemistry (R.Y., S.T., K.M., E.S.-N., M.N., A.I., Y.S.), Graduate School of Pharmaceutical Sciences, and Department of Pharmacology (S.N.), Faculty of Medicine, Kyoto University, Sakyo-ku, Kyoto 606-8501, Japan

Cumulus cells surround the oocyte and regulate the production and assembly of the extracellular matrix (ECM) around the cumulus-oocyte complex for its timely interaction with sperm in the oviduct. We recently found that C-C chemokines such as CCL2, CCL7, and CCL9 are produced and stimulate integrin-mediated ECM assembly in the postovulatory cumulus to protect eggs and that prostaglandin E_2-EP2 signaling in the cumulus cells facilitates fertilization by suppressing this chemokine signaling, which otherwise results in fertilization failure by preventing sperm penetration through the cumulus ECM. However, it remains unknown as to what mechanisms underlie chemokine-induced cumulus ECM assembly. Here we report that inhibition of EP2 signaling or addition of CCL7 augments RhoA activation and induces the surface accumulation of integrin and the contraction of cumulus cells. Enhanced surface accumulation of integrin then stimulates the formation and assembly of fibronectin fibrils as well as induces cumulus ECM resistance to hyaluronidase and sperm penetration. These changes in the cumulus ECM as well as cell contraction are relieved by the addition of Y27632 or blebbistatin. These results suggest that chemokines induce integrin engagement to the ECM and consequent ECM remodeling through the RhoA/Rho kinase/actomyosin pathway, making the cumulus ECM barrier resistant to sperm penetration. Based on these results, we propose that prostaglandin E_2-EP2 signaling negatively regulates chemokine-induced Rho/ROCK signaling in cumulus cells for successful fertilization. **(*Endocrinology* 150: 3345–3352, 2009)**

Actin reorganization regulated by RhoA, a small GTPase, is essential for many cellular processes, including adhesion, migration, and contraction (1, 2). ROCK (also referred as Rho kinase or ROK) is one of the downstream effectors of RhoA signaling that phosphorylates and inactivates the myosin-binding subunit of myosin phosphatase and directly phosphorylates myosin light chain to activate myosin to cross-link actin filaments and generate contractile force (3–6). RhoA/ROCK-mediated signaling influences the interactions between the actin cytoskeleton and integrins to regulate integrin avidity involved in cell shape, adhesive properties, and the assembly of extracellular matrix (ECM) components such as fibronectin (7–9). Although numerous studies have revealed the pivotal roles of RhoA/ROCK signaling in cancer metastasis (10), leukocyte adhesion (11), and lymphocyte homing (12), the roles of RhoA/ROCK-mediated signaling in other physiological processes, particularly in reproduction, remain elusive.

The cumulus oophorus is composed of a group of closely associated granulosa cells that surround the oocyte in the antral follicle and are collectively called cumulus cells (13). In response to a LH surge, the cumulus cells start to produce ECM components, which are deposited into the intercellular space and are stabilized by accessory proteins. This phenomenon is called cumulus expansion. A major component of the ECM produced by the cumulus cells is hyaluronan, which provides the viscoelastic properties of the cumulus oophorus. Other proteoglycans and glycoproteins, such as fibronectin, laminin, and type IV collagen, are also produced by cumulus cells. The expanded cumulus oophorus (cumulus cells and ECM) forms a tight complex with an oocyte and is ovulated together as the cumulus-oocyte complex (COC). During ovulation, the cumulus oophorus protects the oocyte from mechanic stress and proteolytic enzymes present in the follicle and oviduct and directs the oocyte into the oviduct by

ISSN Print 0013-7227 ISSN Online 1945-7170
Printed in U.S.A.

doi: 10.1210/en.2008-1449 Received October 14, 2008. Accepted March 26, 2009.
First Published Online April 2, 2009
* R.Y., S.T., and K.M. contributed equally to this work.

Abbreviations: COC, Cumulus-oocyte complex; ECM, extracellular matrix; FACS, fluorescence-activated cell sorter; FITC, fluorescein isothiocyanate; FSC-height, forward light scatter; hCG, human chorionic gonadotropin; IVF, *in vitro* fertilization; PG, prostaglandin; ROCK, Rho kinase; TUNEL, terminal deoxynucleotidyl transferase-mediated deoxyuridine triphosphate nick end labeling; WT, wild type.

facilitating its capture by the ciliated epithelial cells of the infundibulum and its transport to the fertilization site (14). In the oviduct, the cumulus oophorus facilitates the access of sperm to the oocyte by trapping and selecting sperm for successful fertilization (15). Thus, complex formation of the oocyte, cumulus cells, and ECM is essential for successful fertilization in the oviduct (16). Indeed, recent studies using mice null of several hyaluronan binding proteins show that the cumulus ECM is required for successful fertilization *in vivo*; female mice deficient in these molecules are subfertile due to a loss of the cumulus and ECM (17–20). On the other hand, once sperm reach the COC, the cumulus ECM needs to be disassembled and degraded so that the sperm can find a passage to the oocyte through the ECM layer. Although it has been suggested and is generally believed that the major cumulus ECM component hyaluronan is broken down by sperm motility and their hyaluronidase (16), it remains unknown whether the disassembly of other cumulus ECM components is induced by the force of the sperm alone or also by the action of an autocrine or paracrine factor from the cumulus.

Prostaglandin (PG) E_2, an arachidonate metabolite most abundantly synthesized within the follicle, is a key mediator of the stimulation of ovulation by gonadotropin (21). PGE_2 elicits its functions by acting on four subtypes of the PGE receptor, EP1 to EP4. Upon gonadotropin stimulation, cyclooxygenase-2 (*Ptgs2*), the rate-limiting enzyme of PG biosynthesis, is induced in all types of cells within the follicle (22), and a large amount of PGE_2 is released into the follicular fluid (23). It was shown previously that ovulation is severely impaired in *Ptgs2* null mice (24). Similarly, reduced ovulation rate was reported in mice lacking the PGE receptor EP2 (*Ptger2*), which is expressed in the cumulus cells (25), indicating that the PGE_2-EP2 signaling in the cumulus plays a role in ovulatory processes. Notably, however, *Ptger2*$^{-/-}$ mice showed a higher rate of failure in fertilization than in ovulation; the ovulation number of *Ptger2*$^{-/-}$ mice is 80% of wild-type (WT) mice, whereas the fertilization rate of *Ptger2*$^{-/-}$ mice is about 20% of WT mice. Both *Ptgs2* and *Ptger2* genes are still highly expressed in cumulus cells, even after ovulation. Intriguingly, COCs isolated from the *Ptger2*$^{-/-}$ oviduct show a significant reduction in *in vitro* fertilization with sperm compared with control WT COCs (25), suggesting that PGE_2-EP2 signaling facilitates cumulus ECM disassembly for sperm penetration.

To obtain insight into the mechanism causing fertilization failure in the *Ptger2*$^{-/-}$ cumulus, we recently isolated WT and *Ptger2*$^{-/-}$ cumuli from the oviduct ampulla of mice and compared their gene expression profiles and found increased expression of genes for chemokines such as *Ccl2*, *Ccl7*, and *Ccl9* in *Ptger2*$^{-/-}$ cumuli compared with those of WT cumuli (26). We molecularly dissected the functional consequences of this enhanced chemokine signaling in *Ptger2*$^{-/-}$ cumuli and found that chemokine signaling facilitates compaction of the cumulus by integrin-mediated ECM assembly, which is down-regulated by PGE_2-EP2 signaling for sperm penetration, leading to successful fertilization (26). It remains unknown, however, as to what signaling mechanisms are involved in chemokine-induced assembly of the cumulus ECM. Here we demonstrate that sustained chemokine stimulation due to down-regulation of the PG pathway in cumulus cells activates RhoA-ROCK signaling, which facilitates the formation of actomyosin bundles, surface accumulation of integrins, and excessive ECM assembly, resulting in the capture of sperm by the cumulus cells.

Materials and Methods

Animals and hormone treatment

Ptger2$^{-/-}$ mice with a C57BL/6 genetic background were analyzed (25, 27), and female C57BL/6 mice were used as WT mice. Mice were maintained on a 12-h light, 12-h dark cycle under specific pathogen-free conditions. Follicular growth and ovulation were stimulated in mice at 3 wk of age by the following hormonal regimen: ip injection of 5 IU pregnant mare serum gonadotropin followed 48 h later by ip injection of 5 IU human chorionic gonadotropin (hCG). Alternatively, WT female mice were sc injected with vehicle (0.1 ml of 1% dimethyl sulfoxide in sesame oil) or indomethacin (5 mg/kg; Sigma-Aldrich, St. Louis, MO) simultaneously with the hCG injection. All experimental procedures were approved by the Committee of Animal Research of Kyoto University Faculty of Pharmaceutical Sciences.

Flow cytometry

COCs were collected from oviducts of WT, *Ptger2*$^{-/-}$, vehicle-treated, or indomethacin-treated mice (three to four mice each) at 14 h after hCG injection. Alternatively, COCs were collected from preovulatory follicles of these mice at 8 h after hCG injection. COCs were washed with *in vitro* fertilization (IVF)-fetal bovine serum medium (α-MEM supplemented with 5% fetal bovine serum, 25 mM sodium bicarbonate, 1 mM calcium lactate, 50 U/ml penicillin, and 0.3% BSA) and dispersed with 0.1% hyaluronidase. Dispersed cumulus cells were collected and analyzed by a flow cytometer (FACSCalibur; Becton Dickinson, Lincoln Park, NJ). Data (10,000 events) were acquired for forward light scatter (FSC-height). On the FSC-height histogram, we defined two regions including typical cumulus cell populations, one between channel numbers 120 and 300 as the low FSC-height region (M1) and the other between 600 and 900 as the high FSC-height region (M2) and then used Cell-Quest-Pro software (Becton Dickinson) to calculate the percentage of total events within those regions. For pharmacological analyses (see Fig. 3, A and B), ampullary parts including COCs were incubated with or without 100 ng/ml CCL7 for 3 h. Incubation was performed in the presence of either 1 μg/ml vMIP-II (Genzyme, Cambridge, MA), 10 μM Y27632 (Calbiochem, La Jolla, CA), or 100 μM blebbistatin (Calbiochem) as required. After the incubation, COCs were obtained from the ampulla and subjected to fluorescence-activated cell sorter (FACS) analysis. In all FACS analyses, propidium iodide was added at a final concentration of 16.5 ng/ml.

Terminal deoxynucleotidyl transferase-mediated deoxyuridine triphosphate nick end labeling (TUNEL) staining

The oviductal ampulla including COCs of WT and *Ptger2*$^{-/-}$ mice at 14 h after hCG injection was excised, sectioned, and subjected to TUNEL staining using the Apoptag kit (Chemicon, Temecula, CA) according to the manufacturer's instructions. At this time point, the cells surrounded by hyaluronan in the oviductal lumen consist of only cumulus cells and oocytes (26). Therefore, we examined the histology of adjacent sections (by toluidine blue or hematoxylin-eosin staining) as a reference and regarded cells that were surrounded by hyaluronan and distinguished from ciliated oviductal epithelial cells as cumulus cells.

RhoA activation assays

COCs collected from WT, *Ptger2*$^{-/-}$, vehicle-treated, or indomethacin-treated mice (16 mice each) at 14 h after hCG were subjected to RhoA activation assays (see Fig. 2B). Alternatively, COCs collected from 16 WT mice at 14 h after hCG were incubated in medium with or without

100 ng/ml CCL7 for 10 min. Incubation was performed in the presence of 1 μg/ml vMIP-II (Genzyme) as required (see Fig. 3C). Measurement of the levels of activated RhoA was essentially performed according to the method of Yamaguchi *et al.* (28). Cell lysates were clarified by centrifugation, and the supernatants were incubated with glutathione-Sepharose beads and glutathione S-transferase fused with the Rho-binding domain of Rhotekin (GST-RBD-Rhotekin), and the bound proteins were eluted in Laemmli sample buffer, separated by 12.5% SDS-PAGE, and analyzed by immunoblotting using a monoclonal anti-RhoA antibody (Santa Cruz Biotechnology, Santa Cruz, CA). Blots were detected using a horseradish peroxidase-conjugated goat antimouse IgG antibody and an ECL detection kit (GE Healthcare, Piscataway, NJ). An aliquot [1:20 (vol/vol)] of each sample was loaded to show the amount of total RhoA content as an input for the pull-down assay.

Immunofluorescence analysis

At 14 h after hCG injection, WT, *Ptger2*$^{-/-}$ and indomethacin-treated mice were killed, and 14 μm frozen sections of the ampulla of each oviduct containing COCs were prepared. Sections were fixed in 2.5% formaldehyde and incubated with Texas Red-phalloidin (Molecular Probes, Eugene, OR). For integrin-β1 detection (see Fig. 4A), isolated COCs were incubated simultaneously with an fluorescein isothiocyanate (FITC)-conjugated hamster antirat CD29 antibody at 4 C, washed for 1 h, and fixed with 1% paraformaldehyde in a detergent-free condition. The specificity of the signals detected by the antibody was confirmed by their disappearance when FITC-conjugated hamster IgM (BD PharMingen, San Diego, CA) was used as an isotype control. For fibronectin detection (see Fig. 4C), isolated COCs were incubated with a rabbit antifibronectin antibody (Sigma) and detected with an Alexa488-conjugated antirabbit IgG antibody (Molecular Probes).

Hyaluronidase resistance

Ampullary parts including COCs were incubated with or without 100 ng/ml CCL7 for 3 h. Incubation was performed in the presence of either 1 μg/ml vMIP-II (Genzyme), 10 μM Y27632 (Calbiochem), or 100 μM blebbistatin (Calbiochem) as required. After the incubation, COCs were obtained from the ampulla and incubated in 0.01% hyaluronidase in medium. After incubation for 15 min, the number of oocytes surrounded by several cumulus cell layers was counted.

IVF

IVF was essentially performed as described previously (26). At 14 h after hCG injection, WT mice were killed, and the ampulla of each oviduct containing COCs was excised and incubated with or without 100 ng/ml CCL7 for 3 h. Incubation was performed in the presence of either 1 μg/ml vMIP-II (Genzyme), 10 μM Y27632 (Calbiochem), or 100 μM blebbistatin (Calbiochem) as required. After the incubation, COCs were introduced into a drop of IVF medium equilibrated under the same conditions as for sperm. Medium containing sperm was added to a drop of medium containing oocytes to give a final concentration of 20 sperm/μl. After 1 h of incubation, the morphology of stripped cumulus cells and their interactions with motile sperm were examined.

Statistical analyses

Data are shown as means ± SEM. Comparison of two groups was analyzed by the Student's *t* test. For comparison of more than two groups with comparable variances, one-way ANOVA was performed first. Then the Tukey's test was used to evaluate the pairwise group difference.

Results

Loss of PGE_2-EP2 signaling affects cumulus cell morphology

When we examined the COCs collected from the oviduct, we found that *Ptger2*$^{-/-}$ cumulus cells are different from WT cells

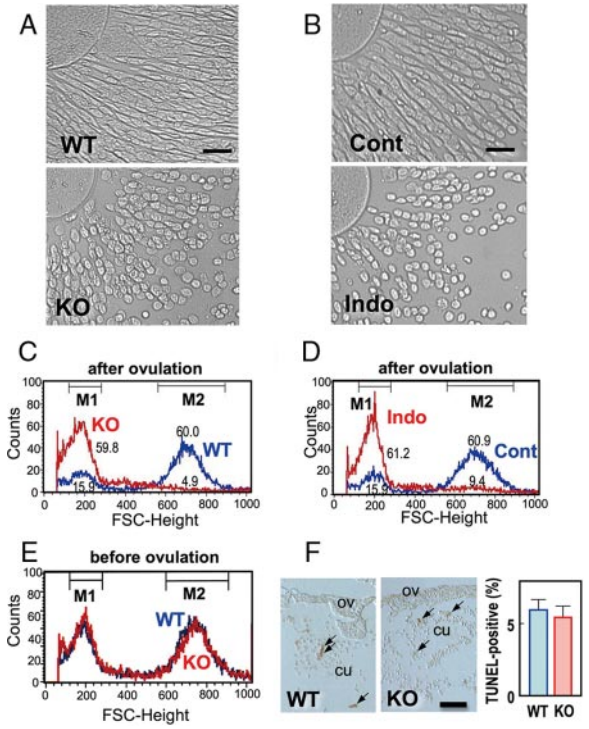

FIG. 1. Cumulus cell rounding in PG signal-depleted oviductal cumuli. A and B, Photomicrographs showing round-shaped cell morphology in oviductal cumuli isolated from WT and *Ptger2*$^{-/-}$ (KO) or from vehicle- (Cont) and indomethacin-treated WT mice (Indo). *Scale bar*, 20 μm. C and D, Cell rounding in oviductal cumuli isolated from *Ptger2*$^{-/-}$ and indomethacin-treated mice analyzed by FACS analysis. The population of cumulus cells from *Ptger2*$^{-/-}$ (KO, *red* in C) and WT mice (WT, *blue* in C) or from indomethacin- (Indo, *red* in C) and vehicle-treated mice (Cont, *blue* in C) are indicated by the FSC-height. Values in the panels show the percentage of cumulus cells contained within the low (M1) and high (M2) FSC-height regions. E, Morphological difference between WT and *Ptger2*$^{-/-}$ (KO) cumulus cells is not observed before ovulation. F, TUNEL staining of oviductal sections (OV) isolated from WT and *Ptger2*$^{-/-}$ (KO) mice at 14 h after hCG injection. TUNEL-positive cumulus cells (CU; *arrows*) were observed in both sections, but their numbers did not differ. *Scale bar*, 50 μm. Representative results of three (A–D) or two (E and F) independent experiments are shown.

in their morphology: WT cumulus cells are angular and spindle shaped, whereas *Ptger2*$^{-/-}$ cumulus cells are round shaped and smaller (Fig. 1A). To quantitatively evaluate the morphological changes in cumulus cells, we performed FACS analysis. WT cells were divided into two groups by size: one group with higher FSC-height, considered to be large and/or complex shaped, and another group with lower FSC-height, considered to be small and/or round shaped. More than 50% of the WT cells showed a high FSC-height (M2), whereas a smaller proportion of cells showed a low FSC height (M1). In *Ptger2*$^{-/-}$ cells, the proportion of cells with a high FSC-height (M2) was dramatically decreased and the major population was shifted to the low FSC-height (M1) (Fig. 1C). This altered morphology of *Ptger2*$^{-/-}$ cumulus cells was apparent only after ovulation and not before ovulation (cumulus cells collected from preovulatory follicles at 8 h, Fig. 1E). There was no significant difference in the populations of propidium iodide-positive cells between WT and *Ptger2*$^{-/-}$ cumulus cells (data not shown), suggesting that such morphological changes in *Ptger2*$^{-/-}$ cells are unlikely to be due to apoptosis. Furthermore, when we performed TUNEL staining of cumulus cells in oviduct sections of WT and *Ptger2*$^{-/-}$ mice

at 14 h after hCG injection, we failed to detect any significant changes in the number of TUNEL-positive cells (Fig. 1F). To examine whether loss of PG signaling around the time of ovulation elicits the morphological changes in cumulus cells, we examined the effect of indomethacin, an inhibitor of PG biosynthesis, on cumulus cell morphology. Indomethacin was administered to mice at the time of hCG injection, COCs were isolated 14 h later, and change in cumulus morphology was examined and assessed by FACS analysis (Fig. 1, B and D). Cell rounding was also observed in cumulus cells isolated from indomethacin-treated mice but not in those from vehicle-treated mice. These results suggested that loss of PG signaling around the time of ovulation causes the altered morphology in *Ptger2*$^{-/-}$ cumulus cells.

Enhanced actin polymerization and RhoA activation in PG signal-depleted cumulus cells

To characterize the molecular changes in *Ptger2*$^{-/-}$ cumulus cells, we examined their actin cytoskeleton. When we stained WT oviductal cumuli with phalloidin, weak fluorescence signals were detected. In contrast, in the *Ptger2*$^{-/-}$ cumuli or indomethacin-pretreated cumuli, prominent ring-like signals were detected around the rounded cell bodies (Fig. 2A). Because the round morphology of *Ptger2*$^{-/-}$ cumulus cells resembles cell contraction induced by activation of the small GTPase RhoA (29, 30), we hypothesized that the round morphology and enhanced actin polymerization of PG signal-depleted cumulus cells is mediated by Rho activation. To test this hypothesis, we examined the amount of the active GTP-bound form of RhoA in COCs, by the Rho-binding domain of Rhotekin pull-down assay, and compared RhoA activation between WT and *Ptger2*$^{-/-}$ COCs. We found that the level of RhoA activation was significantly augmented in the *Ptger2*$^{-/-}$ COCs (Fig. 2B). Moreover, apparent RhoA activation was observed in the COCs isolated from indomethacin-treated mice but not in the COCs from vehicle-treated mice (Fig. 2B). These results indicate that PG signaling endogenously suppresses RhoA activation in the cumulus.

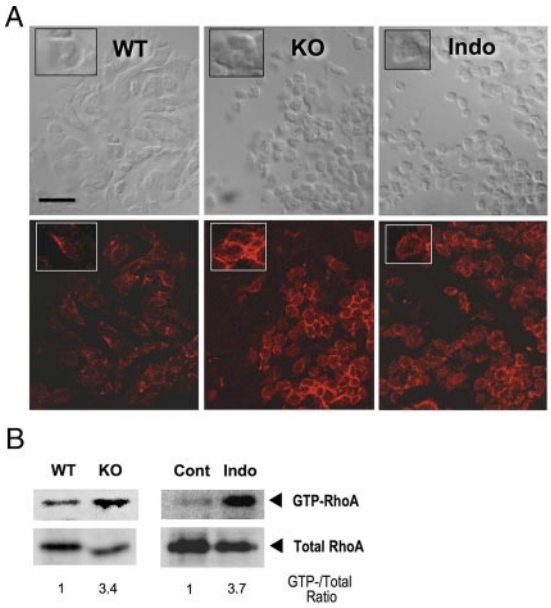

FIG. 2. Loss of PG signaling enhances RhoA activation and actin polymerization. A, F-actin staining of the oviductal cumuli of WT, *Ptger2*$^{-/-}$ (KO) and indomethacin-pretreated WT mice (Indo). The ampulla of oviducts containing COCs was excised at 14 h, and the frozen tissue was transversely sectioned. F-actin staining with Texas Red-X phalloidin (*bottom panels*) and bright-field images of the same section (*top panels*) are shown. *Inset*, Magnified view of typical cell morphology and F-actin staining of the same field. Note that cumulus cell rounding in KO or Indo was associated with prominent ring-like F-actin signals. *Scale bar*, 20 μm. B, Increased RhoA activation in PG signal-depleted COCs. COCs isolated from WT and *Ptger2*$^{-/-}$ (KO) mice at 14 h were subjected to the RhoA pull-down assay (16 mice for each). Similar analysis was also performed between COCs from vehicle- (Cont) and indomethacin-treated mice (Indo). The total RhoA level in each lysate used for the pull-down assay is shown as an input. Note that the levels of total RhoA were relatively reduced in the KO and Indo COCs due to reduced ovulation, but the levels of GTP-RhoA was nevertheless increased in these COCs. The ratio of GTP-RhoA to total RhoA for each sample is also shown. Representative results of two independent experiments are shown.

CCL7 stimulates RhoA activation and contraction in cumulus cells

We recently found that PGE_2-EP2 signaling negatively regulates the expression of chemokine genes such as *Ccl2* and *Ccl7* in WT cumulus cells and that CCR1/CCR2 chemokine signaling is augmented in *Ptger2*$^{-/-}$ cumulus cells (26). We therefore investigated whether augmented chemokine signaling affects cumulus cell morphology. We incubated WT COCs with CCL7, an agonist for both CCR1 and CCR2, for 3 h and then subjected the cumulus cells to FACS analysis (Fig. 3A). Compared with the vehicle-treated cumulus cells, the CCL7-treated cells showed an increased number in the small cell population (M1) and a decreased number in the large cell population (M2). The effects of CCL7 were completely blocked by treatment with an antagonist for both CCR1 and CCR2, vMIP-II (31). These results suggest that activation of CCR1 and/or CCR2 leads to the rounding of cumulus cells. We further found that the effect of CCL7 on cu-

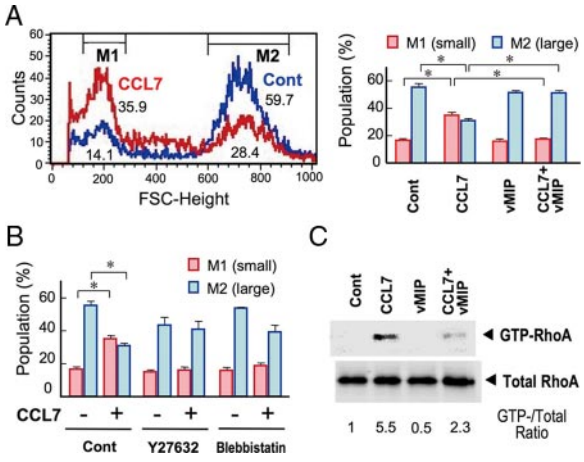

FIG. 3. CCL7 induces cumulus cell rounding by a RhoA-dependent pathway. A, Effect of CCL7 on the size distribution of cumulus cells (*left panel*). COCs were incubated with CCL7 in the presence or absence of vMIP-II for 3 h. Cumulus cells were then subjected to FACS analysis. The percentages of cells within each FSC-height region are also shown as a bar graph (*right panel*). *, $P < 0.01$. B, Effects of Rho pathway inhibitors on CCL7-induced cell contraction. COCs were incubated with CCL7 in the presence of vehicle (Cont), Y27632, or blebbistatin. Cumulus cells were subjected to FACS analysis and the results are shown as a bar graph. *, $P < 0.01$. C, CCL7 induces RhoA activation in COCs. COCs were incubated with CCL7 in the presence or absence of vMIP-II for 10 min and then subjected to the RhoA pull-down assay. Representative results of three (A and B) or two (C) independent experiments are shown.

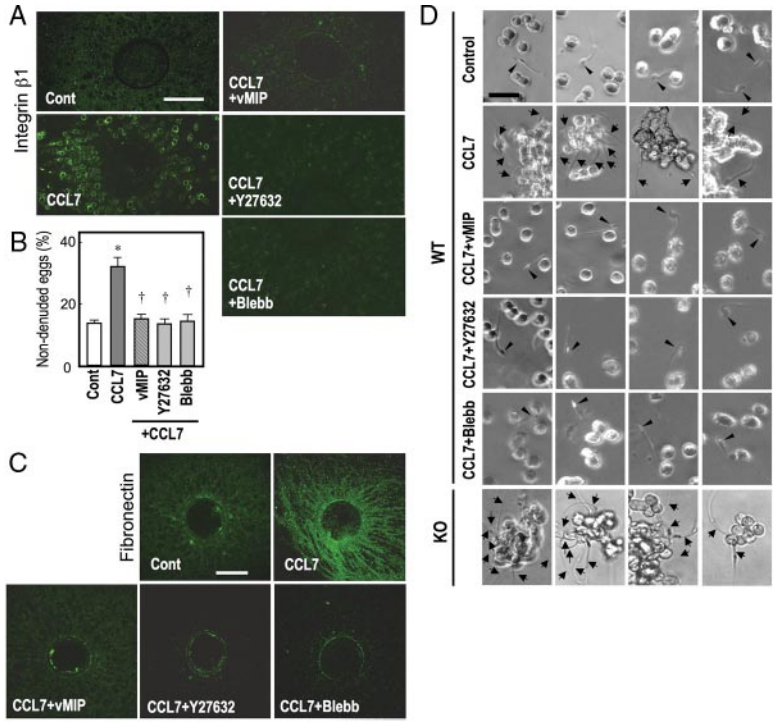

FIG. 4. CCL7 strengthens the cumulus ECM through the Rho/ROCK/actomyosin pathway. The ampulla containing COCs were incubated with CCL7 in combination with vMIP-II (vMIP), Y27632, and blebbistatin (Blebb), and the COCs were excised and analyzed as follows: A, Surface accumulation of integrin-β1 in CCL7-treated cumulus cells. The COCs were stained with an FITC-labeled antimouse integrin-β1 antibody in a nonpermeabilized condition. *Scale bar*, 100 μm. B, CCL7-induced hyaluronidase resistance in the cumulus ECM. The COCs were subjected to 0.01% hyaluronidase treatment. *, $P < 0.01$ (*vs.* Cont); †, $P < 0.01$ (*vs.* CCL7 only). C, CCL7-induced formation and assembly of fibronectin fibrils in the cumulus ECM. The COCs were incubated with a rabbit antifibronectin antibody and detected with an Alexa488-conjugated antirabbit IgG antibody. *Scale bar*, 100 μm. D, CCL7-induced incomplete disassembly of the cumulus ECM and sperm capture by the cumuli during IVF. COCs were incubated with sperm, and their scattering and interaction with sperm were examined. In control COCs, individual cumulus cells were scattered and sperm passed between the cells (*arrowhead*). In CCL7-treated COCs, cumulus cells remained in clusters and a number of sperm (*arrows*) were captured by cumulus cells. Both of the effects of CCL7 were suppressed by vMIP-II, Y27632, and blebbistatin. Four different sperm were examined for control, CCL7+vMIP, CCL7+Y27632, CCL7+blebbistatin, and four different fields were captured for CCL7-treated and *Ptger2*$^{-/-}$(KO) COCs. Representative results of three independent experiments are shown.

mulus morphology was abolished by the ROCK inhibitor Y27632 (32) (Fig. 3B). Because ROCK-induced cell contraction is executed by the induction of ATPase activity of myosin II (6), we then examined the effect of the myosin II inhibitor blebbistatin (33). As a result, blebbistatin inhibited the effect of CCL7 on cumulus cell morphology. To evaluate the effect of CCL7 on RhoA activation in cumulus cells, we performed the Rhotekin pull-down assay. CCL7 augmented the amount of active RhoA in the WT COCs (Fig. 3C). In addition, CCL7-induced RhoA activation was attenuated by vMIP-II (Fig. 3C). These results demonstrate that chemokine-CCR1/CCR2 signaling alters cumulus cell morphology through RhoA activation.

CCL7 strengthens the cumulus ECM assembly through the Rho/ROCK/actomyosin pathway, which prevents sperm penetration

Activation of Rho GTPase induces cell rounding by the induction of actomyosin bundles and integrin clustering on the cell surface (34). Indeed, CCL7 treatment stimulates the surface expression of integrin β1 in cumulus cells, which was also observed in the *Ptger2*$^{-/-}$ or indomethacin-pretreated COCs (26). We therefore explored whether RhoA mediates CCL7-induced integrin activation. As reported previously, *in vitro* CCL7 treatment enhanced the accumulation of integrin-β1 on the cumulus cell surface. This effect of CCL7 was blocked by vMIP-II and abolished by Y27632 and blebbistatin (Fig. 4A). These results demonstrate that CCR1/CCR2 signaling-induced integrin accumulation on the cumulus cell surface is mediated by RhoA/ROCK-mediated activation of actomyosin bundles.

Hyaluronan is a major component of the cumulus ECM and production of hyaluronan induces cumulus expansion (35). Sperm use their own hyaluronidase to penetrate the cumulus ECM layer. We previously demonstrated that CCL7-CCR signaling confers the cumulus ECM with resistance to hyaluronidase through the activation of integrins. We therefore examined the involvement of the RhoA/ROCK/actomyosin pathway in CCL7-induced hyaluronidase resistance of the cumulus ECM. Control COCs or CCL7-treated COCs were exposed to 0.01% hyaluronidase for 15 min and the number of nondenuded eggs was counted. Both control and CCL7-treated COCs responded to hyaluronidase treatment. However, CCL7-treated COCs were significantly more resistant to hyaluronidase than control COCs (Fig. 4B). Moreover, this effect of CCL7 was blocked by vMIP-II and abolished by Y27632 and blebbistatin (Fig. 4B). We further reported that the ECM resistance to hyaluronidase found in WT COCs treated with CCL7 is mediated by the binding of integrin to arginine-glycine-aspartic acid-containing ECM proteins (26, 36). Indeed, fibronectin densely accumulated in the ECM of CCL7-treated COCs, whereas low levels of fibronectin were detected in the ECM of control COCs. Such fibronectin fibril formation by CCL7 was abolished by Y27632 and blebbistatin (Fig. 4C). These results indicated that CCL7-induced hyaluronidase resistance as well as fibronectin fibril formation in the cumulus ECM is mediated through the RhoA/ROCK/actomyosin pathway.

We further examined the appearance of cumuli after incubation of control and CCL7-treated COCs with sperm for 1 h. In control COCs, sperm disassembled the cumulus ECM and the cumulus cells were stripped from the eggs and individually scattered apart from each other (Fig. 4D and supplemental movie 1, published as supplemental data on The Endocrine Society's Journals Online web site at http://endo.endojournals.org). The sperm often came in contact with the dispersed cumulus cells but were able to pass between the cumulus cells. In contrast, in CCL7-treated COCs, most cumulus cells were incompletely dispersed, still forming clusters, indicating that the cumulus ECM showed resistance to sperm hyaluronidase. In addition, a number of motile sperm were trapped by the cumulus cells with their heads adhering to the cumulus surface. This adhesion appeared tight and irreversible because captured sperm were never released (Fig.

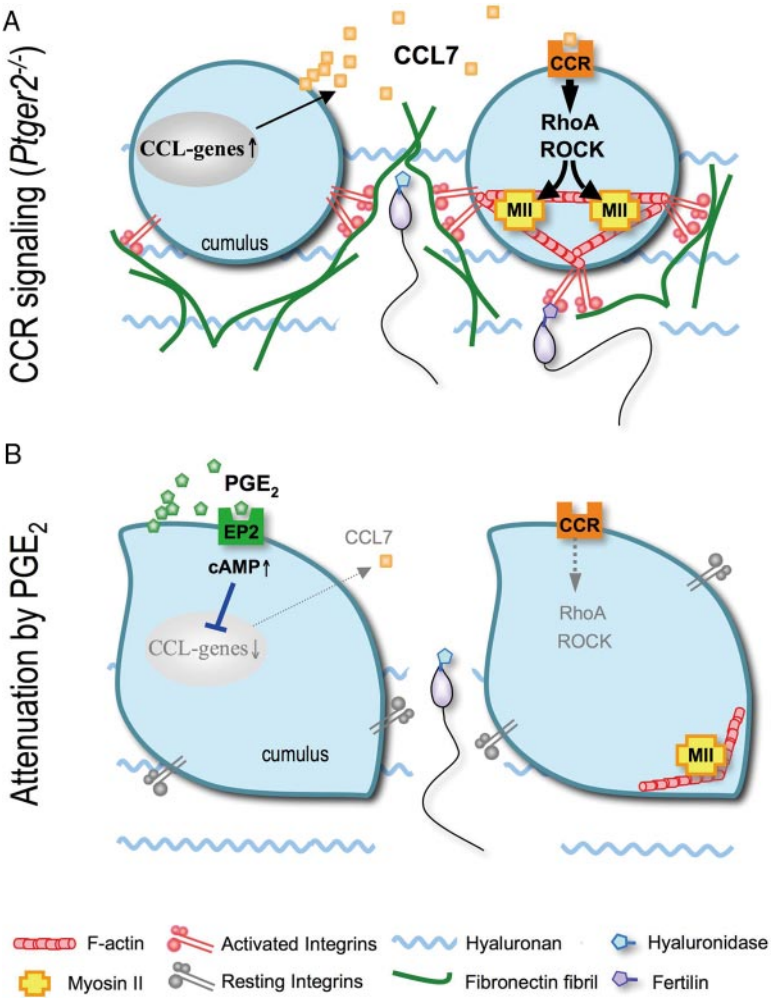

FIG. 5. Schematic model representing the mechanisms underlying the interactions of chemokine and PGE_2 signaling in cumulus ECM remodeling. A, Just after ovulation, some signals (such as IL-1β) stimulate gene expression of chemokines such as CCL7 in the cumulus cells. CCL7, by acting on the cumulus themselves in an autocrine fashion, stimulates RhoA/ROCK activation and actomyosin cross-linking, resulting in cell contraction and the cell surface accumulation of integrins, which enhance fibronectin fibril formation. B, Once the COCs reach the fertilization site, PGE_2/EP2/cAMP signaling attenuates such chemokine actions on the cumuli, and allows sperm penetration. However, in *Ptger2*$^{-/-}$ cumuli (A), chemokine signaling persists and interferes with sperm penetration due to its hyaluronidase resistance and the direct binding between integrins (cumulus) and fertilin (sperm). CCR, CC-chemokine receptor.

4D and supplemental movie 2). Prominent surface expression of integrin-β1 was still detected on the cell surface of such cumulus masses (data not shown). These phenomena were also observed in *Ptger2*$^{-/-}$ COCs (Fig. 4D and supplemental movie 3). Cumulus cluster formation (ECM resistance to hyaluronidase) and sperm capture induced by CCL7 were blocked by vMIP-II, Y27632, and blebbistatin (Fig. 4D and supplemental movies 4–6, respectively), indicating that both phenomena elicited by CCL7 are mediated by the Rho/ROCK/actomyosin pathway.

Discussion

Roles of the Rho-actomyosin pathway in cumulus and integrin-fibronectin assembly

The present study demonstrates that chemokines promote RhoA-mediated actomyosin bundle formation, leading to cell rounding, surface accumulation of integrin, and fibronectin fibril formation. Surface accumulation of integrin is a key event for the interference of sperm penetration. There are two possible mechanisms for the surface expression of integrins: 1) accelerated sorting of integrins from intracellular components to the plasma membrane or 2) accelerated formation of integrin clusters on the plasma membrane. We could not address this issue due to the difficulties in the staining of intact integrins on the cell surface within the cumulus ECM. However, because the Rho-ROCK pathway has been shown to regulate the formation of focal adhesions and integrin clustering (37–40), cell surface accumulation of integrin may reflect enhanced integrin clustering on the cumulus cell surface. Indeed, a number of punctate signals for integrin-β1 and -αv were observed on the cell surface of cumulus cells (26). Another point is whether fibronectin fibril formation results from the enhanced cell surface expression of integrins. Previously Zhong *et al.* (7) reported that GTP-RhoA promotes fibronectin matrix assembly in a cell contraction-dependent and integrin-independent manner: fibronectin assembly is promoted by a tension. Because we observed cumulus cell rounding, it is possible that RhoA-mediated cumulus cell contraction directly stimulates fibronectin assembly, and the resultant fibronectin fibrils may stimulate integrin clustering and integrin-mediated intracellular signaling.

Roles of Rho-ROCK signaling in the cumulus on fertilization

What is the significance of Rho-ROCK signaling in the cumulus cells on fertilization? To directly address this issue, we examined the effect of Y27632 or blebbistatin on the fertilization rate of WT COCs and cumulus-free oocytes. However, both compounds prominently reduced the fertilization rates, even in the absence of cumulus cells (data not shown). These results indicate that ROCK-actomyosin signaling is required for fertilization itself or some machinery that maintains fertilizability in the oocytes. Indeed, Rho-ROCK-mediated actin cytoskeleton remodeling has been shown to play a role in a fertilization-associated event in sea urchin eggs (41). Alternatively, RhoA-mediated formation of an actomyosin gradient has been shown to be critical for polarity formation of fertilized eggs in *Caenorhabditis elegans* (42). Thus, it is likely that Rho-ROCK signaling plays a role also in mammalian fertilization, but the pharmacological approach we used was not fit to address this issue. However, other approaches such as cumulus-specific gene disruption of RhoA signaling molecules will be useful to address the physiological significance of Rho-ROCK signaling in the cumulus cells in fertilization.

In summary, we demonstrated that CCR1/CCR2 signaling stimulates RhoA/ROCK-mediated activation of actomyosin bundles and the cell surface accumulation of integrins in the

cumulus, causing excessive fibronectin assembly in the ECM and sperm capture by the cumulus. These results together with a previous report (26) indicate that the chemokine system enhances integrin-mediated cumulus ECM protein assembly through the Rho/ROCK/actomyosin pathway and PGE_2-EP2 signaling acts as a negative regulator of chemokine actions to induce the appropriate ECM status to allow sperm to penetrate the cumulus ECM layer (Fig. 5). These results contribute to our understanding of not only the mechanism of PGE_2-promotion of fertilization but also the importance of chemokine signaling in the regulation of the cumulus ECM for successful fertilization.

Acknowledgments

We thank Drs. M. Negishi and H. Katoh for kind instruction of the RhoA-Rho binding domain assay and providing Glutathione-S-Transferase-Rhotekin beads. We are grateful to Dr. K. Nakayama in our department for precious advice and continuous support. We are also grateful to Dr. H. A. Popiel and Ms. Y. Nakaminami for careful reading of the manuscript and secretarial assistance, respectively.

Address all correspondence and requests for reprints to: Dr. Yukihiko Sugimoto, Department of Physiological Chemistry, Graduate School of Pharmaceutical Sciences, Kyoto University, Yoshida, Sakyo-ku, Kyoto 606-8501, Japan. E-mail: ysugimot@pharm.kyoto-u.ac.jp.

This work was supported by a research fellowship from the Japan Society for the Promotion of Science for Young Scientists (to S.T.); and Grants-in-Aid for Scientific Research from the Ministry of Education, Culture, Sports, Science, and Technology of Japan (to E.S.-N., A.I., S.N., and Y.S.), the Ministry of Health and Labor of Japan (to Y.S.), and the National Institute of Biomedical Innovation of Japan (to S.N.).

Disclosure Summary: The authors of this manuscript have nothing to declare.

References

1. **Van Aelst L, D'Souza-Schorey C** 1997 Rho GTPases and signaling networks. Genes Dev 11:2295–2322
2. **Etienne-Manneville S, Hall A** 2002 Rho GTPases in cell biology. Nature 420: 629–635
3. **Kimura K, Ito M, Amano M, Chihara K, Fukata Y, Nakafuku M, Yamamori B, Feng J, Nakano T, Okawa K, Iwamatsu A, Kaibuchi K** 1996 Regulation of myosin phosphatase by Rho and Rho-associated kinase (Rho-kinase). Science 273:245–248
4. **Fukata Y, Kimura K, Oshiro N, Saya H, Matsuura Y, Kaibuchi K** 1998 Association of the myosin-binding subunit of myosin phosphatase and moesin: dual regulation of moesin phosphorylation by Rho-associated kinase and myosin phosphatase. J Cell Biol 141:409–418
5. **Feng J, Ito M, Ichikawa K, Isaka N, Nishikawa M, Hartshorne DJ, Nakano T** 1999 Inhibitory phosphorylation site for Rho-associated kinase on smooth muscle myosin phosphatase. J Biol Chem 274:37385–37390
6. **Riento K, Ridley AJ** 2003 ROCKs: multifunctional kinases in cell behaviour. Nat Rev Mol Cell Biol 4:446–456
7. **Zhong C, Chrzanowska-Wodnicka M, Brown J, Shaub A, Belkin AM, Burridge K** 1998 Rho-mediated contractility exposes a cryptic site in fibronectin and induces fibronectin matrix assembly. J Cell Biol 41:539–551
8. **Calì G, Mazzarella C, Chiacchio M, Negri R, Retta SF, Zannini M, Gentile F, Tarone G, Nitsch L, Garbi C** 1999 RhoA activity is required for fibronectin assembly and counteracts β1B integrin inhibitory effect in FRT epithelial cells. J Cell Sci 112:957–965
9. **Worthylake RA, Burridge K** 2003 RhoA and ROCK promote migration by limiting membrane protrusions. J Biol Chem 278:13578–13584
10. **Itoh K, Yoshioka K, Akedo H, Uehata M, Ishizaki T, Narumiya S** 1999 An essential part for Rho-associated kinase in the transcellular invasion of tumor cells. Nat Med 5:221–225
11. **Laudanna C, Campbell JJ, Butcher EC** 1996 Role of Rho in chemoattractant-activated leukocyte adhesion through integrins. Science 271:981–983
12. **Giagulli C, Scarpini E, Ottoboni L, Narumiya S, Butcher EC, Constantin G, Laudanna C** 2004 RhoA and ζPKC control distinct modalities of LFA-1 activation by chemokines: critical role of LFA-1 affinity triggering in lymphocyte *in vivo* homing. Immunity 20:25–35
13. **Matzuk MM, Burns KH, Viveiros MM, Eppig JJ** 2002 Intercellular communication in the mammalian ovary: oocytes carry the conversation. Science 296:2178–2180
14. **Talbot P, Shur BD, Myles DG** 2003 Cell adhesion and fertilization: steps in oocyte transport, sperm-zona pellucida interactions, and sperm-egg fusion. Biol Reprod 68:1–9
15. **Tanghe S, Van Soom A, Nauwynck H, Coryn M, de Kruif A** 2002 Functions of the cumulus oophorus during oocyte maturation, ovulation, and fertilization. Mol Reprod Dev 61:414–424
16. **Primakoff P, Myles DG** 2002 Penetration, adhesion, and fusion in mammalian sperm-egg interaction. Science 296:2183–2185
17. **Zhuo L, Yoneda M, Zhao M, Yingsung W, Yoshida N, Kitagawa Y, Kawamura K, Suzuki T, Kimata K** 2001 Defect in SHAP-hyaluronan complex causes severe female infertility. A study by inactivation of the bikunin gene in mice. J Biol Chem 276:7693–7696
18. **Varani S, Elvin JA, Yan C, DeMayo J, DeMayo FJ, Horton HF, Byrne MC, Matzuk MM** 2002 Knockout of pentraxin 3, a downstream target of growth differentiation factor-9, causes female subfertility. Mol Endocrinol 16:1154–1167
19. **Fülöp C, Szántó S, Mukhopadhyay D, Bárdos T, Kamath RV, Rugg MS, Day AJ, Salustri A, Hascall VC, Glant TT, Mikecz K** 2003 Impaired cumulus mucification and female sterility in tumor necrosis factor-induced protein-6 deficient mice. Development 130:2253–2261
20. **Salustri A, Garlanda C, Hirsch E, De Acetis M, Maccagno A, Bottazzi B, Doni A, Bastone A, Mantovani G, Beck Peccoz P, Salvatori G, Mahoney DJ, Day AJ, Siracusa G, Romani L, Mantovani A** 2004 PTX3 plays a key role in the organization of the cumulus oophorus extracellular matrix and in *in vivo* fertilization. Development 131:1577–1586
21. **Murdoch WJ, Hansen TR, McPherson LA** 1993 A review—role of eicosanoids in vertebrate ovulation. Prostaglandins 46:85–115
22. **Sirois J, Simmons DL, Richards JS** 1992 Hormonal regulation of messenger ribonucleic acid encoding a novel isoform of prostaglandin endoperoxide H synthase in rat preovulatory follicles. Induction *in vivo* and *in vitro*. J Biol Chem 267:11586–11592
23. **Brown CG, Poyser NL** 1984 Studies on ovarian prostaglandin production in relation to ovulation in the rat. J Reprod Fertil 72:407–414
24. **Lim H, Paria BC, Das SK, Dinchuk JE, Langenbach R, Trzaskos JM, Dey SK** 1997 Multiple female reproductive failures in cyclooxygenase 2-deficient mice. Cell 91:197–208
25. **Hizaki H, Segi E, Sugimoto Y, Hirose M, Saji T, Ushikubi F, Matsuoka T, Noda Y, Tanaka T, Yoshida N, Narumiya S, Ichikawa A** 1999 Abortive expansion of the cumulus and impaired fertility in mice lacking the prostaglandin E receptor subtype EP2. Proc Natl Acad Sci USA 96:10501–10506
26. **Tamba S, Yodoi R, Segi-Nishida E, Ichikawa A, Narumiya S, Sugimoto Y** 2008 Timely interaction between prostaglandin and chemokine signaling is a prerequisite for successful fertilization. Proc Natl Acad Sci USA 105: 14539–14544
27. **Kabashima K, Saji T, Murata T, Nagamachi M, Matsuoka T, Segi E, Tsuboi K, Sugimoto Y, Kobayashi T, Miyachi Y, Ichikawa A, Narumiya S** 2002 The prostaglandin E receptor EP4 suppresses colitis, mucosal damage and CD4 cell activation in the gut. J Clin Invest 109:883–893
28. **Yamaguchi Y, Katoh H, Yasui H, Aoki J, Nakamura K, Negishi M** 2000 $G_{\alpha 12}$ and $G_{\alpha 13}$ inhibit Ca^{2+}-dependent exocytosis through Rho/Rho-associated kinase-dependent pathway. J Neurochem 75:708–717
29. **Xu J, Wang F, Van Keymeulen A, Herzmark P, Straight A, Kelly K, Takuwa Y, Sugimoto N, Mitchison T, Bourne HR** 2003 Divergent signals and cytoskeletal assemblies regulate self-organizing polarity in neutrophils. Cell 114: 201–214
30. **Rot A, von Andrian UH** 2004 Chemokines in innate and adaptive host defense: basic chemokinese grammar for immune cells. Annu Rev Immunol 22:891–928
31. **Kledal TN, Rosenkilde MM, Coulin F, Simmons G, Johnsen AH, Alouani S, Power CA, Luttichau HR, Gerstoft J, Clapham PR, Clark-Lewis I, Wells TN, Schwartz TW** 1997 A broad-spectrum chemokine antagonist encoded by Kaposi's sarcoma-associated herpesvirus. Science 277:1656–1659
32. **Uehata M, Ishizaki T, Satoh H, Ono T, Kawahara T, Morishita T, Tamakawa H, Yamagami K, Inui J, Maekawa M, Narumiya S** 1997 Calcium sensitization of smooth muscle mediated by a Rho-associated protein kinase in hypertension. Nature 389:990–994

33. **Straight AF, Cheung A, Limouze J, Chen I, Westwood NJ, Sellers JR, Mitchison TJ** 2003 Dissecting temporal and spatial control of cytokinesis with a myosin II Inhibitor. Science 299:1743–1747
34. **Narumiya S** 2003 Signal transduction underlying cell morphogenesis: editorial overview. J Biochem 134:305–307
35. **Chen L, Russell PT, Larsen WJ** 1993 Functional significance of cumulus expansion in the mouse: roles for the preovulatory synthesis of hyaluronic acid within the cumulus mass. Mol Reprod Dev 34:87–93
36. **Mao Y, Schwarzbauer JE** 2005 Fibronectin fibrillogenesis, a cell-mediated matrix assembly process. Matrix Biol 24:389–399
37. **Ishizaki T, Naito M, Fujisawa K, Maekawa M, Watanabe N, Saito Y, Narumiya S** 1997 p160ROCK, a Rho-associated coiled-coil forming protein kinase, works downstream of Rho and induces focal adhesions. FEBS Lett 404:118–124
38. **Clark EA, King WG, Brugge JS, Symons M, Hynes RO** 1998 Integrin-mediated signals regulated by members of the rho family of GTPases. J Cell Biol 142: 573–586
39. **Schwartz MA, Shattil SJ** 2000 Signaling networks linking integrins and rho family GTPases. Trends Biochem Sci 25:388–391
40. **Rodríguez-Fernández JL, Sánchez-Martín L, Rey M, Vicente-Manzanares M, Narumiya S, Teixidó J, Sánchez-Madrid F, Cabañas C** 2001 Rho and Rho-associated kinase modulate the tyrosine kinase PYK2 in T-cells through regulation of the activity of the integrin LFA-1. J Biol Chem 276:40518–40527
41. **Rangel-Mata F, Méndez-Márquez R, Martínez-Cadena G, López-Godínez J, Nishigaki T, Darszon A, García-Soto J** 2007 Rho, Rho-kinase, and the actin cytoskeleton regulate the Na+-H+ exchanger in sea urchin eggs. Biochem Biophys Res Commun 352:264–269
42. **Jenkins N, Saam JR, Mango SE** 2006 CYK-4/GAP provides a localized cue to initiate anteroposterior polarity upon fertilization. Science 313:1298–1301